Article

Cell Stem Cell

Active and Passive Demethylation of Male and Female Pronuclear DNA in the Mammalian Zygote

Graphical Abstract

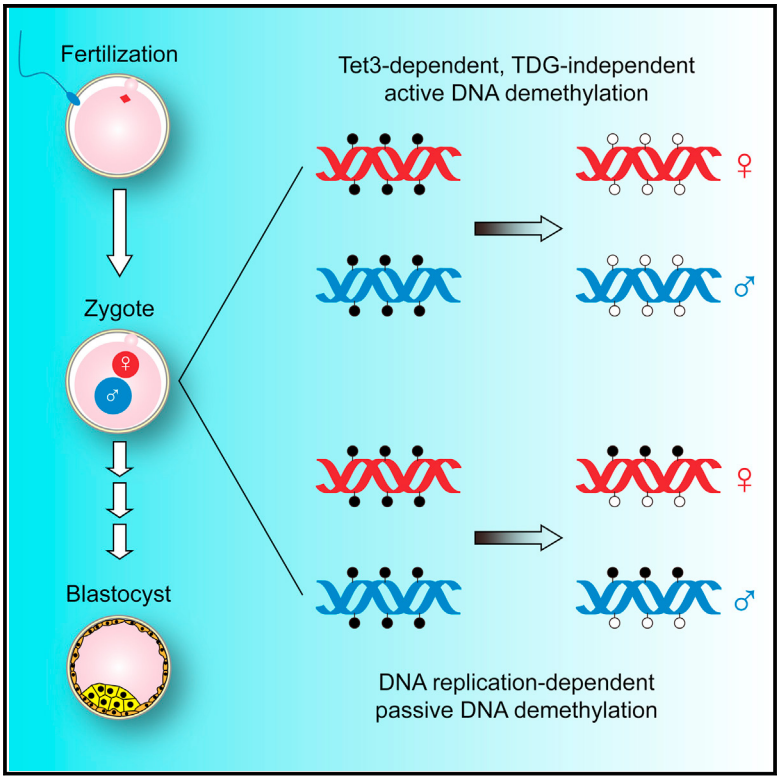

Highlights

Maternal and paternal genomes both undergo active demethylation in mouse zygotes

Both zygotic genomes also undergo replication-dependent passive demethylation

At actively demethylated loci, 5mCs are processed to unmodified cytosines

Active demethylation depends on Tet3 dioxygenase, but not on TDG glycosylase

Authors

Fan Guo, Xianlong Li, ..., Fuchou Tang, Guo-Liang Xu

Correspondence

jsli@sibcb.ac.cn (J.L.), tangfuchou@pku.edu.cn (F.T.), glxu@sibcb.ac.cn (G.-L.X.)

In Brief

In one-cell mouse embryos, the maternal and paternal genomes both undergo global Tet3-dependent active demethylation and replication-mediated passive demethylation. Surprisingly, the active demethylation pathway does not require TDG.

Accession Numbers

GSE56650

Guo et al., 2014, Cell Stem Cell 15, 1–12
October 2, 2014 ©2014 Elsevier Inc.
http://dx.doi.org/10.1016/j.stem.2014.08.003

CellPress

Please cite this article in press as: Guo et al., Active and Passive Demethylation of Male and Female Pronuclear DNA in the Mammalian Zygote, Cell Stem Cell (2014), http://dx.doi.org/10.1016/j.stem.2014.08.003

Cell Stem Cell
Article

Active and Passive Demethylation of Male and Female Pronuclear DNA in the Mammalian Zygote

Fan Guo,[1,2,6] Xianlong Li,[1,6] Dan Liang,[3,6] Tong Li,[2,6] Ping Zhu,[1] Hongshan Guo,[1] Xinglong Wu,[1] Lu Wen,[1] Tian-Peng Gu,[2] Boqiang Hu,[1] Colum P. Walsh,[4] Jinsong Li,[3,*] Fuchou Tang,[1,5,*] and Guo-Liang Xu[2,*]
[1]Biodynamic Optical Imaging Center, College of Life Sciences, Peking University, Beijing 100871, China
[2]State Key Laboratory of Molecular Biology, Shanghai Key Laboratory of Molecular Andrology
[3]Group of Epigenetic Reprogramming, State Key Laboratory of Cell Biology
Institute of Biochemistry and Cell Biology, Chinese Academy of Sciences, Shanghai 200031, China
[4]Centre for Molecular Biosciences, School of Biomedical Sciences, University of Ulster, Coleraine BT52 1SA, UK
[5]Ministry of Education Key Laboratory of Cell Proliferation and Differentiation, Peking University, Beijing 100871, China
[6]Co-first author
*Correspondence: jsli@sibcb.ac.cn (J.L.), tangfuchou@pku.edu.cn (F.T.), glxu@sibcb.ac.cn (G.-L.X.)
http://dx.doi.org/10.1016/j.stem.2014.08.003

SUMMARY

The epigenomes of mammalian sperm and oocytes, characterized by gamete-specific 5-methylcytosine (5mC) patterns, are reprogrammed during early embryogenesis to establish full developmental potential. Previous studies have suggested that the paternal genome is actively demethylated in the zygote while the maternal genome undergoes subsequent passive demethylation via DNA replication during cleavage. Active demethylation is known to depend on 5mC oxidation by Tet dioxygenases and excision of oxidized bases by thymine DNA glycosylase (TDG). Here we show that both maternal and paternal genomes undergo widespread active and passive demethylation in zygotes before the first mitotic division. Passive demethylation was blocked by the replication inhibitor aphidicolin, and active demethylation was abrogated by deletion of Tet3 in both pronuclei. At actively demethylated loci, 5mCs were processed to unmodified cytosines. Surprisingly, the demethylation process was unaffected by the deletion of TDG from the zygote, suggesting the existence of other demethylation mechanisms downstream of Tet3-mediated oxidation.

INTRODUCTION

Postfertilization epigenome reprogramming modulates the outcome of transgenerational inheritance by erasing epigenetic marks transmitted through gametes and creating new marks. In preimplantation mouse embryos, the parental genomes reduce DNA methylation on a global scale. Recently, we and others have shown that in the one-cell zygote, the paternal genome is actively demethylated by Tet3 dioxygenase-dependent oxidation of 5mC (Gu et al., 2011; Iqbal et al., 2011; Wossidlo et al., 2011) while the maternal genome undergoes gradual passive 5mC dilution over subsequent cleavage divisions due to DNA replication (Rougier et al., 1998). The oxidized forms of 5mC, 5-hydroxymethylcytosine (5hmC), 5-formylcytosine (5fC), and 5-carboxylcytosine (5caC) can be passively diluted (Inoue et al., 2011; Inoue and Zhang, 2011). Among them, 5fC and 5caC can also be removed by TDG DNA glycosylase-triggered base excision repair (He et al., 2011; Kohli and Zhang, 2013). These processes collectively result in a hypomethylated genome in the naive pluripotent epiblast cells of the blastocyst (Kobayashi et al., 2012; Smith et al., 2012), which will develop into the whole embryo proper. The epigenetic reprogramming of parental genomes endows the early embryo with developmental potency (Hackett and Surani, 2013; Saitou et al., 2012).

Early work, principally using immunofluorescence with 5mC-specific antibodies, suggested active demethylation in the male pronucleus of mouse zygotes on a global level (Mayer et al., 2000; Santos et al., 2002). The approach used, however, precluded revealing the details of 5mC loss in the two pronuclei and was further confounded by passive 5mC dilution due to pronuclear DNA replication (Wossidlo et al., 2010). A recent study (Wang et al., 2014) characterized the methylation status in mouse gametes and early embryos and concluded that there is active demethylation of both the maternal and paternal methylomes, but it did not examine the methylation status in one-cell zygotes directly or use loss-of-function approaches to study the role of Tet3 or DNA replication. We set out to explore the role of active and passive demethylation directly by looking at pronuclear DNA. To initially define the extent of active demethylation and the targets involved, we extracted both male and female pronuclei individually from one-cell zygotes and determined the methylomes at base resolution on a genome-wide scale using an improved reduced representation bisulfite sequencing (RRBS) approach we recently developed (Guo et al., 2013; Meissner et al., 2005). We further validated the modification states of selected genomic loci using hairpin-bisulfite analysis (Laird et al., 2004) and the newly developed M.SssI-assisted bisulfite (MAB) sequencing method (Hu et al., 2014) that allowed us to distinguish cytosine from its modified forms. In this report, we present direct evidence for Tet3-mediated, but TDG-independent, active DNA demethylation to unmodified cytosines, together with replicative dilution of 5mC in both maternal and paternal genomes during pronuclear zygote development.

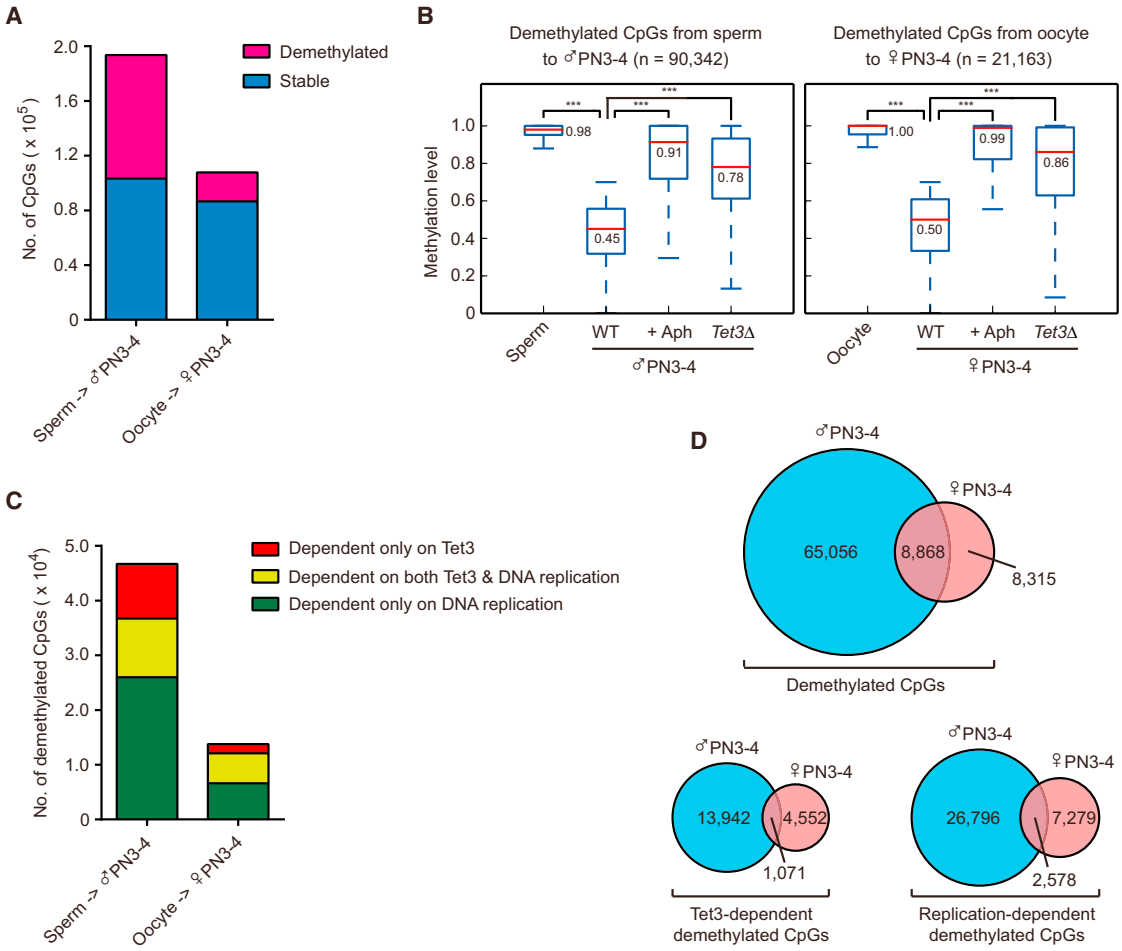

Figure 1. DNA Demethylation in Male and Female Pronuclei of Mouse Zygotes

(A) Total numbers of demethylated sites in the parental genomes after fertilization; 394,252 CpG sites in the paternal genome and 342,622 CpG sites in the maternal genome had at least 5× coverage. Among them 193,608 CpGs (49%) were highly methylated in the sperm and 107,711 CpGs (31%) were highly methylated in the oocyte (methylation level $\geq$ 0.75); 90,342 CpGs (47%) were significantly demethylated from sperm to male pronuclei, and 21,163 CpGs (20%) were significantly demethylated from oocyte to female pronuclei (demethylation level $\geq$ 0.3, $p < 0.05$, FDR < 0.05).

(B) Box plots of the demethylated CpG sites in the paternal and maternal genomes. For CpGs losing methylation in the paternal genome, the median level decreased from 0.98 in sperm to 0.45 in WT male pronuclei. However, the level was 0.91 in the aphidicolin treated male pronuclei and 0.78 in those from Tet3-deficient zygotes. For CpGs losing methylation in the maternal genome, the median level drops from 1.00 in oocyte to 0.50 in WT female pronuclei. However, it stays at 0.99 in the aphidicolin treated female pronuclei and 0.86 in the female pronuclei from Tet3-deficient zygotes, indicating that a significant proportion of demethylation depends on the Tet3-mediated active mechanism. Red lines indicate the median, edges stand for the 25th and 75th percentile, and whiskers extend to the most extreme data point within the [1.5 × (75%–25%)] data range. Data were analyzed using t test.

(C) Tet3-mediated active demethylation versus replication-mediated passive demethylation in male and female pronuclei. A paternally demethylated CpG site is called Tet3 dependent when the methylation level of the CpG site returns to a level comparable to that in the sperm ($\leq$0.05 methylation level difference between sperm and the Tet3 knockout male pronuclei). Similar criteria were applied for the aphidicolin (+Aph) dependence test in male pronuclei and for both Tet3 and Aph dependence tests in the female pronuclei.

(D) Comparison of demethylated CpGs between maternal and paternal genomes. Note that the CpGs analyzed here were the ones covered at least 5× in both paternal and maternal genomes.

RESULTS

Methylome Analysis of Female and Male Pronuclear DNA Reveals Comprehensive Locus-Specific Demethylation

We isolated individual pronuclei from mouse zygotes at the late pronuclear stages PN3–PN4, made pools containing either female or male pronuclei, and used an RRBS method that had been validated for analysis of small numbers of cells (Figure S1 available online). Compared with oocytes and sperm, both the maternal and paternal zygotic DNA displayed widespread, but site-specific, reduction of methylation, with 90,342 and 21,163 CpG sites demethylated in male and female pronuclei, respectively (Figure 1A). As paternal genome demethylation in the male pronucleus requires Tet3-mediated hydroxylation of 5mC (Gu et al., 2011; Wossidlo et al., 2011), we examined the effect of Tet3 deletion on methylome reprogramming. Indeed, in Tet3-deficient zygotes (*Tet3*Δ), a substantial proportion (44%)

of the CpG sites demethylated in the WT male pronucleus (20,698 of 46,685) at least partially retained the methylation seen in sperm (Figures 1B and 1C; $p < 0.001$). To our surprise, in the female pronucleus 7,174 out of 13,778 (52%) demethylated CpG sites also showed impaired demethylation (Figure 1B and 1C; $p < 0.001$), identifying sites wholly or partially dependent on active demethylation in the maternal genome.

The first DNA replication is known to take place from late PN3 up to early PN5 stages (Wossidlo et al., 2010). To assess the contribution of replication-dependent passive loss to demethylation, we next analyzed pronuclear DNA from zygotes treated with the replication inhibitor aphidicolin (Aph). The effect of aphidicolin treatment was confirmed on the basis of the absence of EdU incorporation into the pronuclei in zygotes (Figure S2). With inhibition of DNA replication, 36,724 CpG sites in the male pronucleus and 12,076 sites in the female pronucleus were either not demethylated or significantly less demethylated, thus identifying those subject to replication-dependent passive demethylation (Figures 1B and 1C). The actual scale of Tet3- or replication-dependent demethylation might be considerably more extensive as the RRBS analysis only covered 2.2% of the total CpG sites (with at least 5× coverage). Significant fractions of actively and passively demethylated CpG sites overlap between male and female pronuclei (Figure 1D), potentially suggesting a common mechanism underlying demethylation in the two parental genomes.

About 42% of the demethylated CpG sites were found to be clustered at 7,677 genomic loci (68 bp in average length with $\geq$ 4 demethylated CpGs) widely spread over all the mouse chromosomes (Figure 2A). Both the active and passive demethylation loci are more enriched at intergenic regions in the paternal genome compared with those in the maternal genome (Figure 2B). These biases may be a response to the higher overall levels of intergenic methylation previously noted in sperm compared with oocytes (Kobayashi et al., 2012; Smallwood et al., 2011). It is noteworthy that demethylation of 527 loci (25.3%) in the male pronucleus and 64 loci (13.3%) in the female pronucleus depended primarily on Tet3 (and were independent of DNA replication), as exemplified by *Mbtd1*, *Zbtb32* (Figure 2C), and *1700067k01Rik* (Figure S3), while demethylation of 1,281 paternal and 265 maternal loci mainly depended on replication as shown for the *Sox2ot* and *Fam108a* loci (Figure 2D). In support of enzymatic demethylation in both parental genomes, the Tet3 protein was detected in each pronucleus, albeit with a lower abundance (Figure 3A) and correlating with fewer oxidation products (5hmC and 5caC) in the female pronucleus (Figures 3B and 3C).

Demethylation on Both Strands of the Pronuclear DNA

An active mode of demethylation should result in the removal of 5mC on both cytosines in a CpG dyad (5′CG3′/3′GC5′), whereas passive demethylation due to DNA replication should give rise to a hemimethylated state (5′mCG3′/3′GC5′) (Ooi and Bestor, 2008; Seisenberger et al., 2013). To examine whether loss of 5mC takes place on both complementary strands in pronuclear DNA, we performed hairpin-bisulfite sequencing analysis for a few selected genomic loci, in which the 5′ and 3′ strand ends of genomic restriction fragments were ligated with a stem-loop oligonucleotide to covalently link the two complementary strands within a double-stranded DNA molecule prior to denaturing and bisulfite conversion (Laird et al., 2004). Our previous work demonstrated Tet3-mediated demethylation in the promoter region of *Nanog* in the male pronucleus (Gu et al., 2011). Consistent with this, hairpin-bisulfite analysis revealed a substantial loss of 5mC on both strands in this region in male pronucleus, compared with the hypermethylation state in sperm (Figure 4, left). We reasoned that the promoter of *Dnmt3b* might undergo active demethylation in female pronucleus because it was methylated in oocytes but unmethylated in ESCs (Figure S4) and two-cell stage embryos (Smith et al., 2012). The loss of 5mC was indeed predominantly from both strands on a large proportion of the genomic templates examined in the female pronucleus (Figure 4, right). As controls, the imprinted loci *Peg1* and *Gtl2* instead showed maintenance of 5mC on both strands at most CpG dyads (Figure 4), as expected (Hirasawa et al., 2008; Nakamura et al., 2012; Smith et al., 2012). Verifying passive demethylation at some loci, hemimethylation was seen instead at the majority of demethylated sites for most templates at the *Sox2ot* locus (Figure 4), consistent with the replication-dependent mechanism shown by the RRBS data (Figure 2D). Notably, *B1* and *LINE-1* repeats were also mainly subjected to replicative demethylation, as suggested by the formation of numerous hemimethylated CpG dyads in male pronucleus (Figure S5A) and confirmed by blocking replication using aphidicolin (Figure S5B).

Development and Validation of the Methyltransferase M.SssI-Assisted Bisulfite Sanger Sequencing Method to Distinguish Unmodified Cytosine from 5fC and 5caC

Bisulfite treatment followed by PCR amplification results in the conversion of 5-formylcytosine (5fC), 5-carboxylcytosine (5caC) (He et al., 2011; Ito et al., 2011), or unmodified cytosine (C) to thymine (T), while 5mC and 5hmC are resistant to base conversion and give C following PCR amplification. Therefore, the apparent loss of 5mC we are seeing may reflect the generation of 5fC or 5caC rather than C at the loci being examined: to address this we used our recently developed M.SssI-assisted bisulfite Sanger sequencing (MAB Sanger-seq) technique (Hu et al., 2014) to help distinguish C from 5fC and 5caC. Of the three bases, only unmodified cytosine (C) can be methylated by the bacterial CpG methyltransferase M.SssI, so the proportion of bases represented by C can be determined by comparing the MAB Sanger-seq profile with a conventional bisulfite Sanger sequencing (BS Sanger-seq) profile (Figure 5A). To verify the detection principle, a test PCR DNA fragment was methylated using M.SssI in vitro. The appearance of 5mCs at CpG sites were confirmed by bisulfite sequencing (Figure 5B). The resulting 5mCs were then oxidized to 5caC by treatment using purified Tet enzymes. MAB Sanger-seq results indicated as expected the formation of 5caC on the specific test DNA, but not on the control λ DNA (Figure 5C).

To further demonstrate the applicability of MAB Sanger-seq to small amounts of genomic DNA, we examined 5fC or 5caC at the *Dnahc2* and *EpCAM* loci in mouse ESCs using less than 5 ng of genomic DNA. These two loci were chosen because they show relative enrichment of 5fC in ESCs deficient in TDG as determined in a chemically assisted bisulfite sequencing (fCAB-seq) assay by Chuan He's lab (Song et al., 2013). Consistent with this, our MAB Sanger-seq indeed revealed the existence of 5fC

Please cite this article in press as: Guo et al., Active and Passive Demethylation of Male and Female Pronuclear DNA in the Mammalian Zygote, Cell Stem Cell (2014), http://dx.doi.org/10.1016/j.stem.2014.08.003

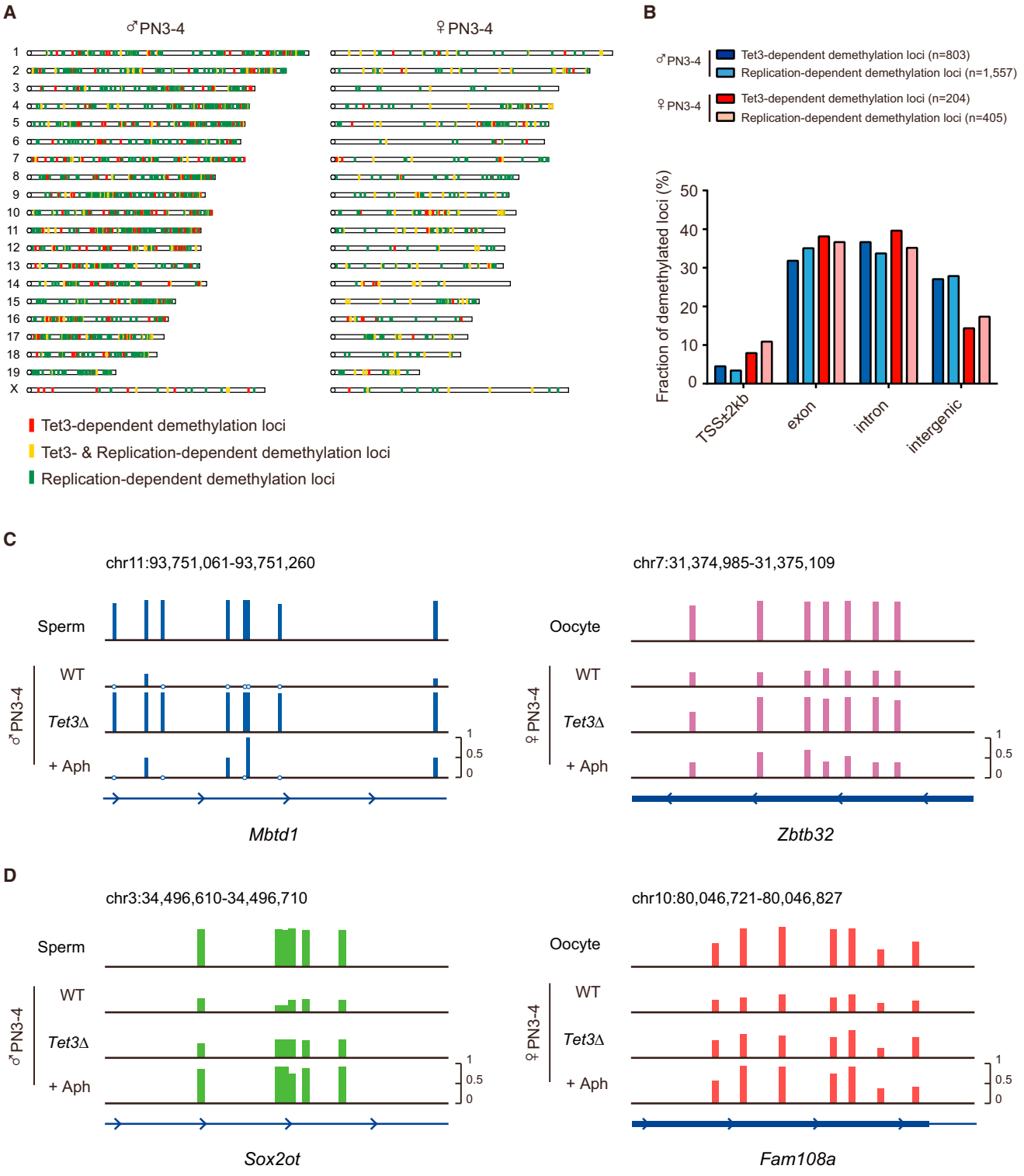

Figure 2. Genome Distribution of Demethylated Loci in Male and Female Pronuclei of Mouse Zygotes

(A) The distribution of demethylated loci on the mouse chromosomes. Note that the Tet3-dependent (or DNA replication-dependent) demethylated loci are widespread across the whole genome.

(B) The distribution of demethylated loci relative to gene features. In the paternal genome, Tet3-dependent (or DNA replication-dependent) loci are more enriched at intergenic regions ($p = 2.2 \times 10^{-5}$ and 2.5×10^{-4}, respectively) compared with those in the maternal genome. Data were analyzed using Pearson's chi-square test.

(legend continued on next page)

or 5caC specifically in *Tdg* knockout cells, thus validating the method for limiting amounts of DNA (Figure 5D).

Conversion of 5mC to Unmodified Cytosine at Specific Genomic Loci in Pronuclear DNA

Having demonstrated that MAB Sanger-seq allows us to distinguish unmodified cytosine from 5fC and 5caC, we next applied this method to evaluate the extent of demethylation at selected genomic loci undergoing active demethylation in zygotes. *Nanog* appeared unmethylated in oocyte (1.1%), hypermethylated in sperm (92.3%), and substantially demethylated in male PN3–PN4 (26.4%) by conventional BS Sanger-seq (open circles in Figure 6, left). To determine if any unmethylated cytosines in male pronucleus could represent 5fC or 5caC, we performed MAB Sanger-seq in parallel, and all sites were found to be bisulfite resistant upon M.SssI treatment (blue circles in Figure 6, right), confirming that they are in fact unmodified cytosines. Similarly, the demethylated sites seen in female pronucleus at the maternally methylated genes *Dnmt3b* and *Zbtb32* were indeed largely unmodified cytosines (Figure 6). The formation of cytosines in pronuclear DNA was also demonstrated for additional demethylated loci (Figure S6A), all of which were initially identified by RRBS except for *Oct4*. The absence or scarcity of detectable 5fC and 5caC in the examined pronuclear DNA loci suggested that these intermediates only exist transiently and were removed rapidly to generate cytosines.

Deletion of TDG Does Not Affect DNA Demethylation

As might be expected, the generation of cytosines at the actively demethylated *Oct4* and *Nanog* loci was unaffected in aphidicolin-treated zygotes (Figure S6B). These observations suggest replication-independent enzymatic conversion of 5mC to C at these genomic loci during pronuclear zygote development. We and others recently showed that excision of 5fC and 5caC by TDG is a downstream event in the Tet-mediated oxidation of 5mC leading to active demethylation (He et al., 2011; Kohli and Zhang, 2013). *Tdg* deletion in mouse results in misexpression of developmental genes, aberrant genomic methylation, and embryonic lethality (Cortázar et al., 2011; Cortellino et al., 2011). As shown above (Figure 5D) and elsewhere (He et al., 2011; Song et al., 2013), *Tdg* mutant ESCs also show an accumulation of 5fC or 5caC both globally and at specific loci. Although *Tdg* expression was not detected during spermatogenesis (Gan et al., 2013), its expression in developing oocytes is unclear. To examine whether TDG participates in oxidative demethylation in fertilized oocytes, we performed germline-specific gene inactivation driven by TNAP-Cre expressed in embryonic germ cells from E9.5 onward. Mouse breeding tests showed no significant change in reproduction in either sex of the conditional knockout (CKO) mice, as evident in the litter size statistics of CKO females (Figure 7A), despite the highly efficient deletion of the *Tdg* allele from germ cells (Figure S7). The relative 5mC, 5hmC, and 5caC signal strength in the pronuclei detected by immunostaining did not appear different in the zygotes lacking maternal TDG when compared with wild-type controls (Figure 7B). Additionally, the conversion of 5mC to unmodified cytosine proceeded normally at the paternally methylated *Oct4* and the maternally methylated *Zbtb32* loci, with no increase in 5fC and 5caC levels (Figure 7C). These data indicate that TDG is dispensable for the zygotic demethylation process, as well as germ cell and pronuclear zygote development.

DISCUSSION

Our methylome analysis of separately isolated female and male zygotic pronuclear DNA demonstrates active removal of methylation and restoration of unmodified cytosine at specific genomic loci of both parental genomes in one-cell embryos. The occurrence of active demethylation soon after fertilization may have benefits for early embryonic development by overcoming the following shortcomings of passive demethylation: (1) passive demethylation through DNA replication does not lead to erasure of DNA methylation completely, but retains the original methylation on the parental strands. Although retained hemimethylation becomes diluted out, this state may still prevent binding of transcription factors and repress transcriptional activation on some chromosomes in early embryos; (2) hemimethylated sites could be mistakenly remethylated in blastomeres when the Dnmt1 methyltransferase is functional (Howell et al., 2001; Li and Sasaki, 2011). Dnmt1 may not be able to discriminate the hemimethylated sites formed by passive zygotic demethylation from those becoming hemimethylated during the latest rounds of DNA replication and may thus restore full methylation to passively demethylated sites. Excessive methylation, if it occurs, would result in insufficient expression of key genes such as *Oct4* or *Nanog*, compromising the developmental potency of the embryo (Gu et al., 2011).

Both active and passive demethylation occur widely in the mouse genome. While demethylation of some of these loci depends on both Tet3 and DNA replication, others rely on just one of these mechanisms. For example, Tet3-mediated active demethylation occurs at the *Oct4* and *Nanog* loci and is unaffected when DNA replication is blocked (Figure S6B). The fact that both actively and passively demethylated sites are more abundant in the paternal DNA may account for the observation of 5mC loss preferentially in the male pronucleus in previous studies, many of which were based on immunohistochemical staining (Reik et al., 2001).

The extent of zygotic active demethylation might have been underestimated for two reasons. First, sites scored as 5mC in PN3–PN4 zygotes may in fact have been 5hmC, as these cannot

(C) Representative loci showing Tet3-dependent active demethylation in male (*Mbtd1*, 8 CpGs shown; read coverage 24×) and female (*Zbtb32*, 7 CpGs shown; read coverage 568×) pronuclei, respectively. Vertical bars indicate the methylation level (0–1) at individual CpG dyads (counting the two complementary CpGs). An open circle in place of a bar means the CpG was detected as unmethylated. Note that in the absence of Tet3 (*Tet3*Δ), methylation reduction is compromised at most CpG sites. Without DNA replication (+Aph), demethylation is still largely achieved.

(D) Representative loci showing DNA replication-dependent passive demethylation in male (*Sox2ot*, an intergenic genomic locus on chromosome 9, 6 CpGs shown; read coverage 83×) and female (*Fam108a*, 7 CpGs shown; read coverage 102×) pronuclei, respectively. Note that in the absence of DNA replication (+Aph), the gametic level of methylation is maintained at all CpG sites. *Tet3* deletion does not interfere with the methylation decrease caused by replication-based passive dilution.

Please cite this article in press as: Guo et al., Active and Passive Demethylation of Male and Female Pronuclear DNA in the Mammalian Zygote, Cell Stem Cell (2014), http://dx.doi.org/10.1016/j.stem.2014.08.003

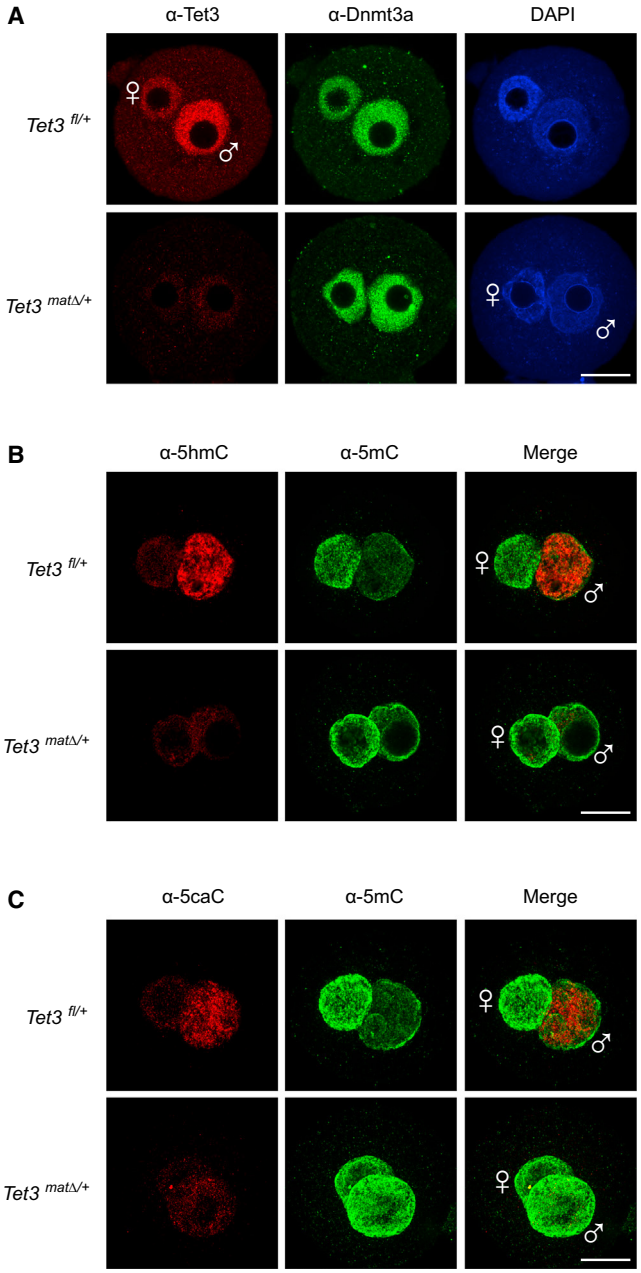

Figure 3. Distribution of the Tet3 Protein and 5mC Oxidation Products in Mouse Zygotes

(A) Confirmation of Tet3 protein distribution in the female and male pronuclei of wild-type zygotes and its absence in mutant zygotes derived from *Tet3*-deleted oocytes. Immunostaining was performed using a Tet3 antibody specific for the deleted protein region. The signal from the female pronucleus in WT zygotes (*fl*/+, top row), albeit weaker than that of the male pronucleus, is significantly and reproducibly above the background level, as validated by comparison with *Tet3*-knockout (*mat Δ*/+) control zygotes (bottom row). The scale bar represents 25 μm.

(B) Loss of 5hmC signal (red) in the pronuclei of Tet3-deficient zygotes. Refer to Gu et al. (2011) for more information. The scale bar represents 25 μm.

(C) Loss of 5caC signal (red) in the pronuclei of Tet3-deficient zygotes. Shown are representative images. Refer to Experimental Procedures for antibody performance validation. The scale bar represents 25 μm.

be discriminated by conventional bisulfite sequencing. Second, the demethylation process might not be complete until PN5, by which stage female and male pronuclei are getting too close to be separated physically. The notion of more comprehensive zygotic demethylation is also supported by previous observations that the paternally hypermethylated *Nanog* locus and the maternally hypermethylated *Dnmt3b* locus are largely free of methylation in the two-cell and cleavage stage embryos (Smith et al., 2012).

During the revision of our manuscript, another group reported active demethylation of the maternal genome after the two-cell stage (Wang et al., 2014). However, they did not directly examine active demethylation in one-cell stage pronuclei or look at the functional role of Tet3 or TDG in this process. Their raw data on the maternal genome also show low levels of overall methylation at maternally imprinted alleles relative to other reports (around 75% versus around 95% expected) (Kobayashi et al., 2012; Xie et al., 2012) and the existence of unexpectedly high levels of methylation at paternally imprinted alleles (15%–46% versus around 5%), raising the possibility that there was significant contamination of the oocyte and two-cell embryo samples used with a somatic DNA source such as cumulus cells.

Crucially, we demonstrate an active demethylation process that requires Tet3-mediated oxidation and encompasses the conversion of 5mC to unmodified cytosine. The yet-to-be identified mechanism downstream of Tet3 can potentially involve decarboxylation of 5caC (Schiesser et al., 2012), dehydroxymethylation of 5hmC (Chen et al., 2012), or base excision repair (Hajkova et al., 2010; Santos et al., 2013; Wossidlo et al., 2010), but it is clearly independent of the thymine DNA glycosylase TDG that otherwise can feed the oxidation (5fC and 5caC) or putative deamination products of 5mC into the base excision repair pathway (He et al., 2011; Seisenberger et al., 2013).

While in the zebrafish embryo paternal methylation is stably maintained and the relatively hypomethylated maternal genome undergoes drastic reprogramming to establish a spermlike methylome (Jiang et al., 2013; Potok et al., 2013), both parental genomes in the early mouse embryo appear to undergo global demethylation to create a hypomethylated epigenome of the inner cell mass by the blastocyst stage. Recent analyses of the human DNA methylome during embryonic development indicate that the global methylation change in human zygotes is very similar to that in mouse (Guo et al., 2014; Smith et al., 2014), suggesting a conservation of mechanistic aspects of mammalian DNA demethylation as revealed in this study. Stella (Dppa3 or PGC7) has been reported to protect some loci from Tet3-mediated oxidation in mouse zygotes (Bian and Yu, 2014; Nakamura et al., 2007, 2012; Wossidlo et al., 2011). However, further studies are required to address both the functional significance and molecular processes of embryonic DNA demethylation, particularly in the contexts of intergenerational inheritance and creation of zygotic totipotency.

EXPERIMENTAL PROCEDURES

Animal Use and Care

Animal procedures were carried out according to the ethical guidelines of the Institute of Biochemistry and Cell Biology, Shanghai Institutes for Biological Sciences, Chinese Academy of Sciences.

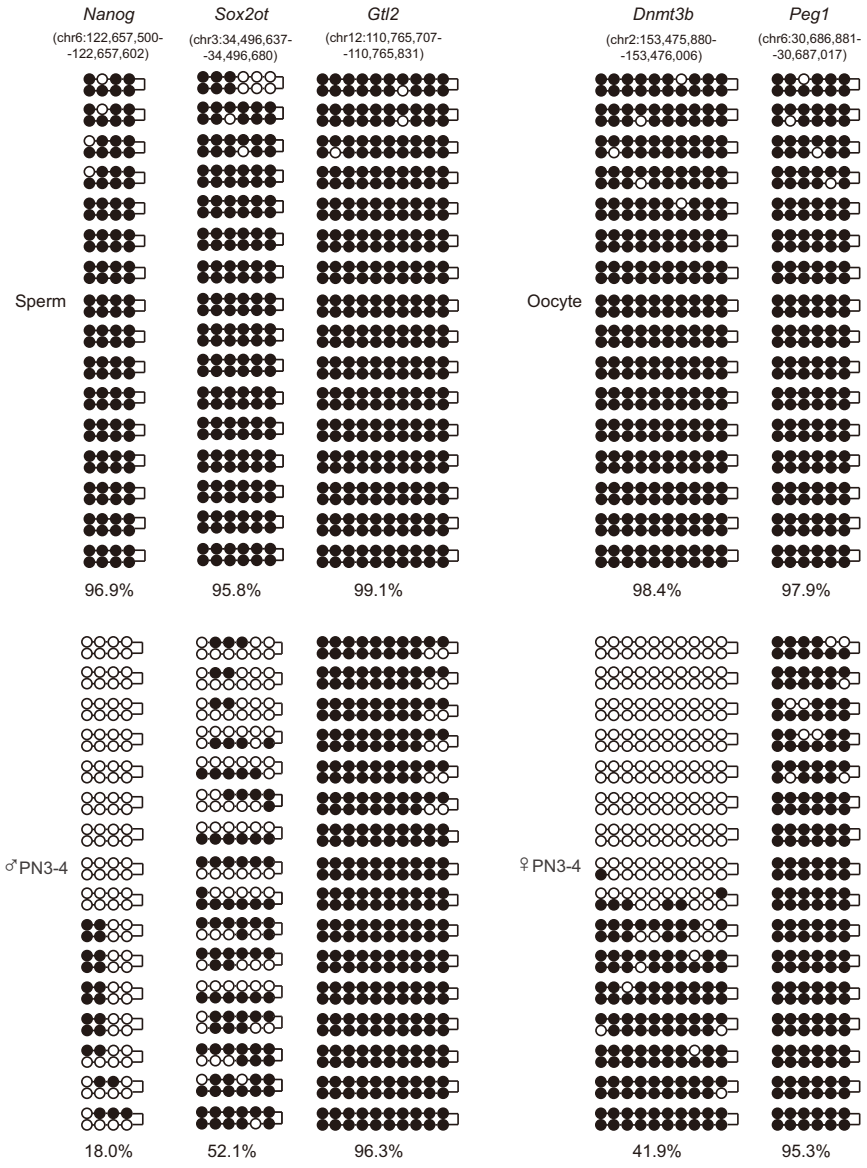

Figure 4. Hairpin-Bisulfite Sanger Sequencing Analysis of Complementary Strands at Specific Genomic Loci

Note that the paternally hypermethylated *Nanog* and the maternally hypermethylated *Dnmt3b* show methylation loss (or are oxidized to 5fC or 5caC) on both strands in the corresponding pronucleus. The paternally methylated *Sox2ot* loses methylation only from one strand at many sites. By contrast, the paternally imprinted *Gtl2* and maternally imprinted *Peg1* genes retain methylation at their differentially methylated regions on both strands. Biological replicates of pronuclear DNA isolated from 100–150 male or female pronuclei produced consistent data. Slight differences in methylation patterns among clones confirm the absence of substantial amplification or clonal bias. See also Figure S5.

Collection of PN3–PN4 Mouse Zygotes

One-cell zygotes were collected 7.5–8 hr after intracytoplasmic sperm injection. Their pronuclear stages were further determined on the basis of microscopic observation of the size of the two pronuclei and the distance between them. Zygotes [*Tet3 mat⊿*/+] deficient in maternal Tet3 were obtained using Zp3-Cre conditional knockout female mice as previously described (Gu et al., 2011). Zygotes deficient in TDG were obtained by TNAP-Cre mediated deletion of the conditional allele (He et al., 2011) (Figure S7). For inhibition of pronuclear DNA replication, zygotes were incubated with 0.2 μg/ml of aphidicolin until the extraction of pronuclei. The effect of aphidicolin treatment was validated through prevention of EdU incorporation into DNA (Figure S2) (assayed using a click-iT EdU Alexa Fluor 488 Imaging Kit (Invitrogen) according to the manufacturer's protocol) and blockage of passive demethylation at *LINE1* (Figure S5B).

Isolation of Pronuclei

Male pronuclei, which were distinguished from female pronuclei on the basis of their size and distance from the polar bodies, were first harvested from zygotes of PN3–PN4 stages by breaking the zona using a Piezo drive (Prime Tech) and aspirating using a micromanipulator. Female pronuclei were extracted afterward. For conventional bisulfite analysis, 40–60 pronuclei were used. For MAB and hairpin-bisulfite sequencing analysis, 80–150 pronuclei were used. For RRBS analysis, 100–130 pronuclei were used for each biological replicate. The possibility of contamination from the opposite pronucleus or other sources was ruled out by the confirmation of the expected methylation state at the imprinted loci using combined bisulfite restriction analysis (COBRA; data not shown). The purity of the female pronuclei was further verified by the fact that in the RRBS data from 100–130 female pronuclei, a paternally imprinted gene locus (*H19*) was essentially free of DNA methylation as expected (Figure S1B). Similarly, the purity of the male pronuclei was further verified by the fact that in the RRBS data from 100–130 male pronuclei, two maternally imprinted gene loci (*Gnas* and *Peg1/Mest*) were essentially free of DNA methylation as expected (Figure S1C).

Reduced Representation Bisulfite Sequencing

The RRBS was performed following the protocol we recently developed (Guo et al., 2013). Approximately 100–130 pronuclei were harvested and pooled together for each experiment and lysed in 5 μl lysis buffer (20 mM Tris, 2 mM EDTA, 20 mM KCl, 0.3% Triton X-100, 1 mg/ml QIAGEN protease) at 50°C for 3 hr. Protease was inactivated at 75°C for 30 min. About 0.1% of unmethylated lambda DNA was added as spike-in to analyze the efficiency of bisulfite conversion. Genomic DNA from pronuclei was digested by 10 U TaqI (NEB) for 3 hr at 65°C. Then the digested DNA was end repaired and dA tailed with exonuclease-deficient Klenow Fragment (Fermentas) in the presence of 40 μM dATP, 4 μM dGTP, and 4 μM dCTP. Next, Illumina TruSeq adapters were ligated to the DNA fragments using concentrated T4 DNA ligase (Fermentas) overnight. After that, bisulfite conversion of the library was performed using a MethylCode DNA Methylation Kit (Invitrogen). Then bisulfite-converted DNA was amplified by 20 cycles of PCR using PfuTurbo Cx polymerase (Agilent Technologies) and purified by AMPure XP beads (Beckman). Finally, an extra round of PCR amplification was performed to increase the amount of DNA to about 500 ng with a Phusion HF Master Mix (NEB), and the 200~500 bp DNA fragments were selected on a 12% polyacrylamide gel. The libraries were analyzed by a Fragment Analyzer (Advanced Analytical Technologies) to check the fragment size distribution, and those that passed quality control were sequenced on an Illumina HiSeq 2000 or 2500. Illumina adaptor sequences were trimmed from the raw sequence reads. Two more bases, which were artificially filled in at the end-repair step,

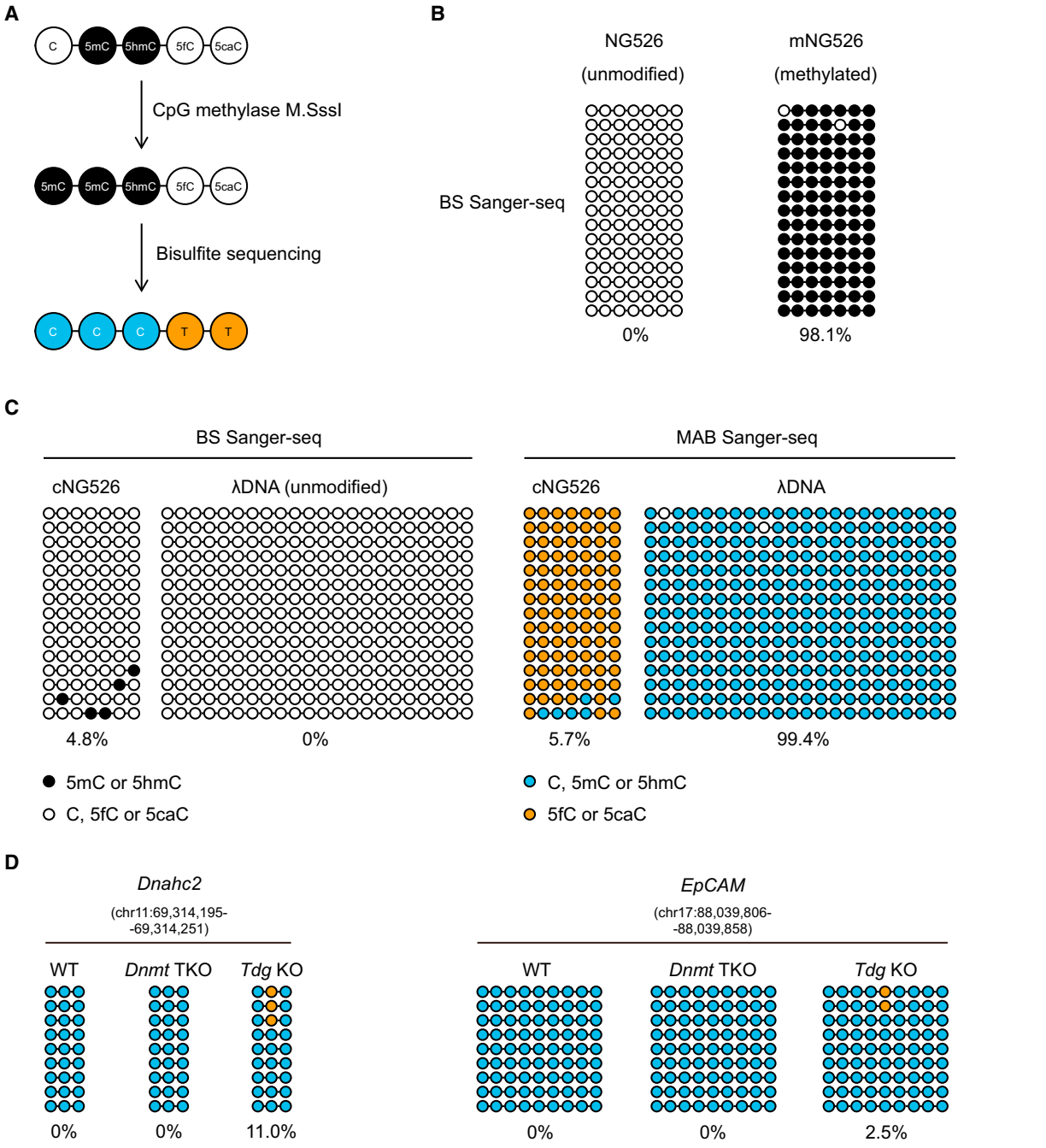

Figure 5. Validation of the M.SssI-Assisted Bisulfite Sanger Sequencing Method

(A) Illustration of the MAB Sanger-seq procedure. A DNA sample is treated with the bacterial CpG methyltransferase M.SssI in vitro to methylate—and thus protects all unmodified CpG sites—prior to bisulfite treatment, which converts 5fC and 5caC into 5fU and 5caU. Consequently, 5fC and 5caC are read as "C" due to their conversion to "T" (orange fill), while all other forms (5mC, 5hmC, and C) in the original sample are read as "5mC" (black fill) due to their maintenance as "C" during PCR amplification and sequencing analysis.

(B) Confirmation of 5mC formation on an M.SssI-treated test DNA fragment by bisulfite sequencing analysis. The PCR fragment of 526 bp (NG526) was methylated in vitro using M.SssI, giving mNG526, which was further oxidized using Tet1 enzymes. The resulting cNG526 DNA showed nearly complete conversion of 5mC to 5caC in a base composition analysis by high-performance liquid chromatography (data not shown).

(C) BS and MAB Sanger sequencing profiles demonstrating the ability to distinguish 5fC or 5caC from other cytosine species. Oxidized test DNA cNG526 and unmodified λ DNA were analyzed. The λ DNA has unmodified CpGs, which appear as T on bisulfite conversion as usual, but if methylated by M.SssI prior to bisulfite treatment they become resistant and appear as C (blue circles) in the MAB products. 5caC (or 5fC) in cNG526 appear as T in both BS Sanger-seq (open circles) and in MAB Sanger-seq (orange circles) as they can be bisulfite converted but cannot be modified by M.SssI. The two white circles in λ DNA MAB-seq may represent CpGs escaping M.SssI methylation.

(D) Detection of 5fC and 5caC (orange) at the *Dnahc2* and *EpCAM* genomic loci in *Tdg*-knockout mouse ESCs. Shown are MAB Sanger-seq profiles.

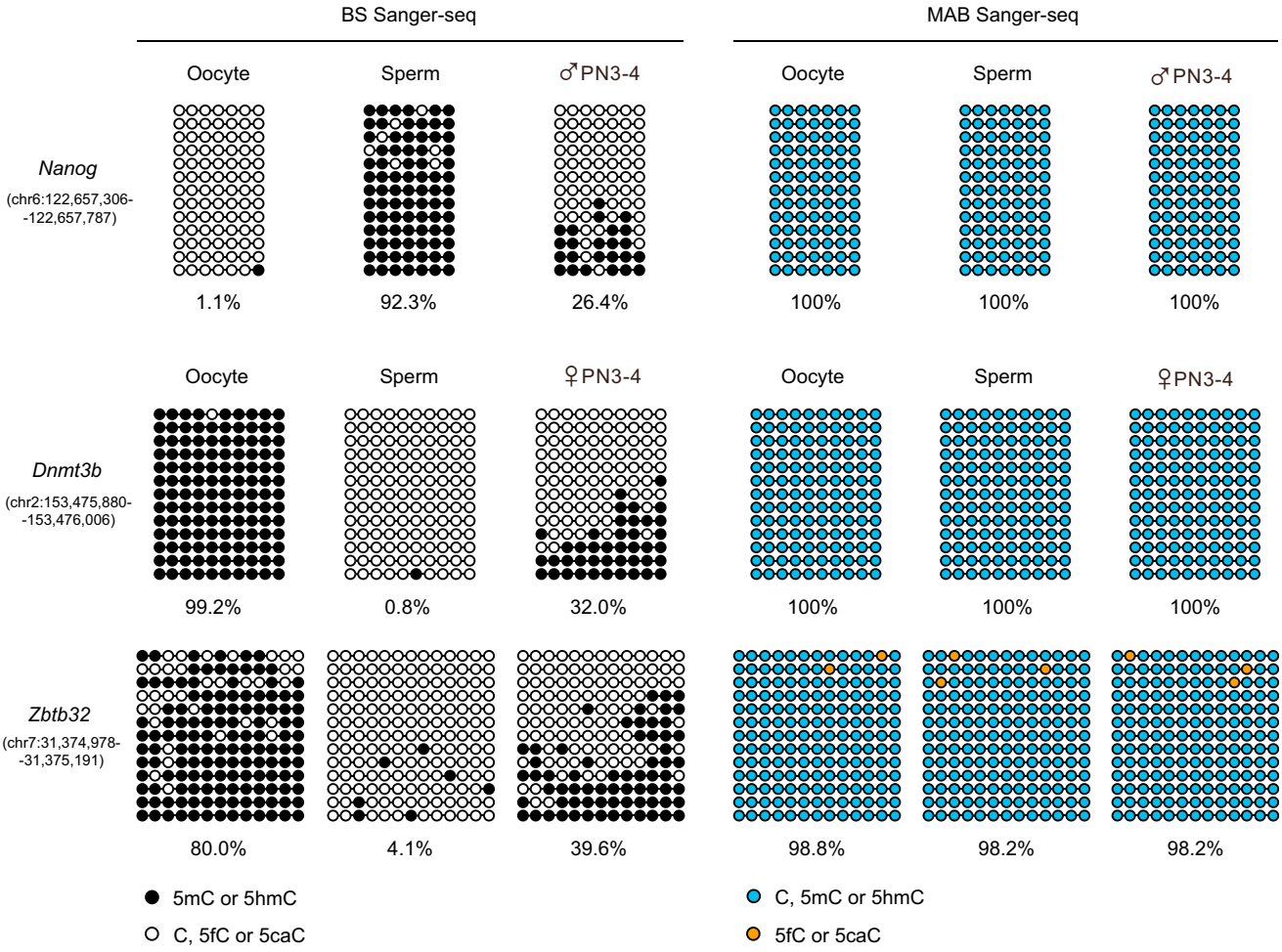

Figure 6. Detection of Unmodified Cytosines at the *Nanog*, *Dnmt3b*, and *Zbtb32* Genomic Loci in Late Pronuclei

Shown are profiles of BS Sanger-seq (left) and MAB Sanger-seq (right). The analyzed genomic regions show high levels of 5mC or 5hmC in sperm or oocytes by BS Sanger-seq (filled circles), but the majority of sites are read as 5fC or 5caC or C (open circles) in the corresponding pronucleus. No 5fC or 5caC were detected following MAB Sanger-seq at *Nanog* and *Dnm3b* and very few at *Zbtb32* (orange circles), which verifies that these sites have been fully demethylated to unmodified cytosines in PN3–PN4 pronuclear DNA. Biological replicates of pronuclear DNA isolated from 80–100 male or female pronuclei produced consistent data. See Figure S6 for other loci analyzed.

were removed from the 3′ end of C → T converted reads and the 5′ end of G → A converted reads. Then the adaptor-trimmed reads were mapped to the mouse genome (mm9) using Bismark (v. 0.76, http://www.bioinformatics.babraham.ac.uk/projects/bismark/). The bisulfite conversion rate was estimated according to the cytosine remnant in the spike-in lambda DNA.

Analysis of RRBS Data: Quantification of DNA Methylation Level

We first calculated the methylation level of each single CpG site using the number of RRBS-measured C (methylated) divided by the sum of measured C (methylated) and T (unmethylated). CpG sites with at least five uniquely mapped reads were chosen for further analysis. We identified individual demethylated CpG sites in wild-type male (or female) pronuclei by comparing the methylation levels to sperm (or oocyte) using the one-tailed Fisher's exact test with $p < 0.05$, with Benjamini-Hochberg false discovery rate (FDR) < 0.05. The methylation level of each CpG site in sperm (or oocyte) not only had to be higher than 0.75 but also had to be demethylated more than 0.3 in the wild-type male (or female) pronuclei. The neighboring demethylated CpG sites were merged to form a demethylated locus if there was at most one CpG site between these two demethylated CpG sites and the distance between them was less than 100 bp.

A Tet3-dependent paternally demethylated CpG site was defined as a site whose pronuclear methylation level rose close to the sperm level (with methylation difference being ≤ 0.05 from the Tet3 knockout pronuclei). Similarly, a Tet3-dependent maternally demethylated CpG site was defined as a site whose methylation level rose to a level comparable to that in the oocyte (i.e., with ≤ 0.05 difference). Criteria for aphidicolin treated samples were the same. The Tet3-dependent or DNA replication-dependent demethylation loci were further manually curated to remove potential false positives.

Conventional Bisulfite Sequencing

For bisulfite sequencing, genomic DNA was treated with an EZ DNA Methylation-Direct Kit (Zymo Research) according to the manufacturer's instructions. Bisulfite-treated DNA was subjected to PCR amplification. The PCR primer sequences are listed in Table S3. The bisulfite primers for the *Oct4* proximal enhancer and *Nanog* promoters were described previously (Gu et al., 2011; Li et al., 2007). For sequencing analysis, PCR products were purified with a Gel Extraction Kit (QIAGEN) and cloned into pMD19-T vectors (Takara). Individual clones were sequenced by standard Sanger sequencing. Data were analyzed by an online methylation tool named BISMA (Rohde et al., 2010)

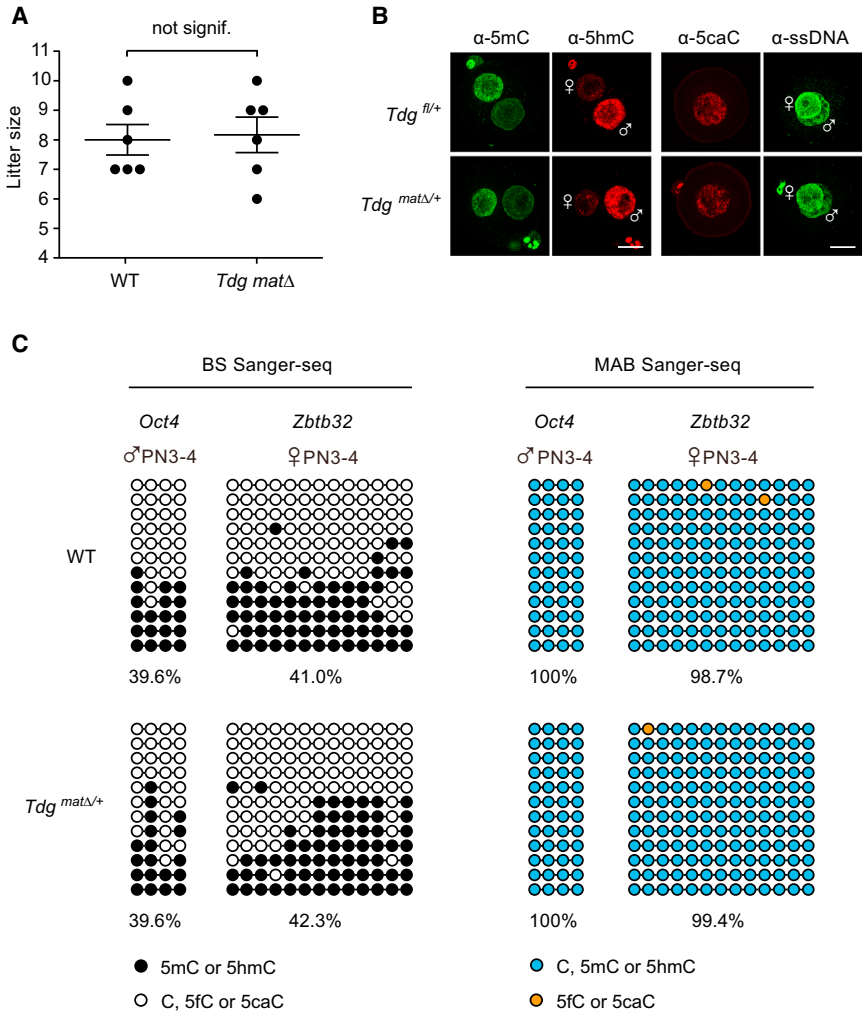

Figure 7. Deletion of TDG Does Not Affect Mouse Reproduction and Zygotic DNA Demethylation

(A) Maternal germline deletion of the *Tdg* gene in the [$Tdg^{fl/-}$, TNAP-Cre] conditional knockout (CKO) female did not affect litter size. Error bars indicate SEM. WT mice, n = 3; *Tdg* CKO mice, n = 3. Each dot represents a litter from which the number of pups were counted and shown at the y axis.

(B) Unaltered 5mC, 5hmC, and 5caC levels in the pronuclear DNA of *Tdg*-deficient zygotes. Shown are representative DNA immunofluorescence images of late pronuclear zygotes. The scale bar represents 20 μm. ssDNA, single-stranded DNA.

(C) Unaffected demethylation at the paternal *Oct4* and maternal *Zbtb32* alleles in maternal *Tdg*-deficient zygotes as revealed by BS Sanger-seq and MAB Sanger-seq analyses of pronuclear DNA. The analyzed regions of *Oct4* and *Zbtb32* are hypermethylated in sperm and oocytes, respectively (Figures S6 and 2). Note that 5fC and 5caC do not accumulate at the analyzed genomic loci in zygotes lacking TDG. See also Figures 6, S6, and S7 for further controls.

(http://services.ibc.uni-stuttgart.de/BDPC/BISMA/), and duplicated clones were deleted by this software. Primer pairs and PCR conditions were tested using a mixture of small amounts of oocyte and sperm genomic DNA or ESC genomic DNA to ensure unbiased recovery of unmethylated and methylated templates.

Hairpin-Bisulfite Sequencing Analysis

Hairpin-bisulfite sequencing analysis of sperm DNA and repetitive sequences in the pronuclear DNA was performed as described (Laird et al., 2004). For analysis of single copy genes, the following modifications were made prior to conventional bisulfite analysis (see above): genomic DNA was cleaved with appropriate restriction enzymes and subsequently treated with Klenow to fill in the ends and generate a single "A" overhang at the 3′ ends of the DNA strands. Then the fragments were ligated with T4 DNA ligase to a hairpin oligonucleotide [stem (16 bp)-loop (5 nucleotides; sequence: GGGCCTATA TAGTATAGGCCCT)] carrying a single "T" overhang at the end of the stem region. Pronuclear DNA was isolated from 100–150 pooled female or male pronuclei. The methylation levels determined by bisulfite sequencing were consistent with the quantification by COBRA (data not shown). Sequencing data were analyzed by BISMA.

M.SssI-Assisted Bisulfite Sanger Sequencing

Genomic DNA was mixed with 0.1% (w/w) of methylation-free lambda DNA (*dam*$^-$, *dcm*$^-$) and methylated by M.SssI (NEB) following the vendor's instruction manual for the complete methylation of treated DNA. Bisulfite conversion, sequencing, and analysis were performed as described above. Full protection of CpGs in the spiked lambda DNA from bisulfite conversion indicated complete in vitro methylation with M.SssI. Synthetic DNA containing 5caC and 5fC was added as an internal control to monitor the complete conversion by the bisulfite treatment. Mouse genomic DNA from *Dnmt* TKO embryonic stem cells lacking DNA methylation (Tsumura et al., 2006), and thus containing no 5fC or 5caC, was used as negative control.

Immunostaining for Tet3, 5hmC, and 5caC in Zygotes

Immunofluorescence detection of the Tet3 protein in zygotes and the 5hmC or 5caC oxidation products in pronuclear DNA was performed following the published procedures (Gu et al., 2011). The generation and performance of the anti-5caC antibody was as described for anti-5hmC (Gu et al., 2011): this is now commercially available through Diagenode (catalog no. C15410204). Anti-Tet3 and anti-Dnmt3a antibodies were as described in our previous publication (Gu et al., 2011). The monoclonal anti-5mC (Catalog No. 39649) and polyclonal anti-5hmC (catalog no. 39791) antibodies were purchased from Active Motif. The monoclonal anti-single-stranded DNA antibody (catalog no. MAB3868) was purchased from Millipore. In general, antibody specificity against a particular DNA modification in cell staining was validated using HEK293T cells transfected with Tet2 and further verified using mouse zygotes deficient in Tet3. Signal suppression was obtained by the addition of a correspondingly modified oligonucleotide into the antibody incubation.

ACCESSION NUMBERS

The Gene Expression Omnibus accession number for the RRBS data reported in this manuscript is GSE56650.

SUPPLEMENTAL INFORMATION

Supplemental Information for this article includes seven figures and four tables and can be found with this article online at http://dx.doi.org/10.1016/j.stem.2014.08.003.

AUTHOR CONTRIBUTIONS

G.-L.X., J.L., and F.T. conceived the project; F.G., T.L., and T.-P.G. designed and performed the methylation analyses; and D.L. and X.W. conducted mouse-embryo-related experiments. X.L., P.Z., H.G., L.W., and B.H. analyzed the methylome data, and G.-L.X., C.P.W., J.L., and F.T. wrote the manuscript.

ACKNOWLEDGMENTS

We thank Xin Sun for critical reading of the manuscript and Lin Li for providing the *Tdg* conditional knockout mouse. This work was supported by grants from the Ministry of Sciences and Technology of China (2012CB966903 and 2014CB964802), the National Science Foundation of China (31230039 and 31221001), the "Strategic Priority Research Program" of the Chinese Academy of Sciences (XDA01010301), and the National Science and Technology Major Project of China (2014ZX09507-002) to G.-L.X.. F.T. was supported by grants from the Ministry of Sciences and Technology of China (2012CB966704 and 2011CB966303) and the National Science Foundation of China (31322037 and 31271543). J.L. was supported by grants from the "Strategic Priority Research Program" of the Chinese Academy of Sciences (XDQ01010403) and the National Science Foundation of China (31225017 and 91319310). C.P.W. was supported by a grant from the Medical Research Council (MR/J007773/1).

Received: April 11, 2014
Revised: June 27, 2014
Accepted: August 15, 2014
Published: September 11, 2014

REFERENCES

Bian, C., and Yu, X. (2014). PGC7 suppresses TET3 for protecting DNA methylation. Nucleic Acids Res. *42*, 2893–2905.

Chen, C.C., Wang, K.Y., and Shen, C.K. (2012). The mammalian de novo DNA methyltransferases DNMT3A and DNMT3B are also DNA 5-hydroxymethylcytosine dehydroxymethylases. J. Biol. Chem. *287*, 33116–33121.

Cortázar, D., Kunz, C., Selfridge, J., Lettieri, T., Saito, Y., MacDougall, E., Wirz, A., Schuermann, D., Jacobs, A.L., Siegrist, F., et al. (2011). Embryonic lethal phenotype reveals a function of TDG in maintaining epigenetic stability. Nature *470*, 419–423.

Cortellino, S., Xu, J., Sannai, M., Moore, R., Caretti, E., Cigliano, A., Le Coz, M., Devarajan, K., Wessels, A., Soprano, D., et al. (2011). Thymine DNA glycosylase is essential for active DNA demethylation by linked deamination-base excision repair. Cell *146*, 67–79.

Gan, H., Wen, L., Liao, S., Lin, X., Ma, T., Liu, J., Song, C.X., Wang, M., He, C., Han, C., and Tang, F. (2013). Dynamics of 5-hydroxymethylcytosine during mouse spermatogenesis. Nat. Commun. *4*, 1995.

Gu, T.P., Guo, F., Yang, H., Wu, H.P., Xu, G.F., Liu, W., Xie, Z.G., Shi, L., He, X., Jin, S.G., et al. (2011). The role of Tet3 DNA dioxygenase in epigenetic reprogramming by oocytes. Nature *477*, 606–610.

Guo, H., Zhu, P., Wu, X., Li, X., Wen, L., and Tang, F. (2013). Single-cell methylome landscapes of mouse embryonic stem cells and early embryos analyzed using reduced representation bisulfite sequencing. Genome Res. *23*, 2126–2135.

Guo, H., Zhu, P., Yan, L., Li, R., Hu, B., Lian, Y., Yan, J., Ren, X., Lin, S., Li, J., et al. (2014). The DNA methylation landscape of human early embryos. Nature *511*, 606–610.

Hackett, J.A., and Surani, M.A. (2013). Beyond DNA: programming and inheritance of parental methylomes. Cell *153*, 737–739.

Hajkova, P., Jeffries, S.J., Lee, C., Miller, N., Jackson, S.P., and Surani, M.A. (2010). Genome-wide reprogramming in the mouse germ line entails the base excision repair pathway. Science *329*, 78–82.

He, Y.F., Li, B.Z., Li, Z., Liu, P., Wang, Y., Tang, Q., Ding, J., Jia, Y., Chen, Z., Li, L., et al. (2011). Tet-mediated formation of 5-carboxylcytosine and its excision by TDG in mammalian DNA. Science *333*, 1303–1307.

Hirasawa, R., Chiba, H., Kaneda, M., Tajima, S., Li, E., Jaenisch, R., and Sasaki, H. (2008). Maternal and zygotic Dnmt1 are necessary and sufficient for the maintenance of DNA methylation imprints during preimplantation development. Genes Dev. *22*, 1607–1616.

Howell, C.Y., Bestor, T.H., Ding, F., Latham, K.E., Mertineit, C., Trasler, J.M., and Chaillet, J.R. (2001). Genomic imprinting disrupted by a maternal effect mutation in the Dnmt1 gene. Cell *104*, 829–838.

Hu, X., Zhang, L., Mao, S.-Q., Li, Z., Chen, J., Zhang, R.-R., Wu, H.-P., Gao, J., Guo, F., Liu, W., et al. (2014). Tet and TDG mediate DNA demethylation essential for mesenchymal-to-epithelial transition in somatic cell reprogramming. Cell Stem Cell *14*, 512–522.

Inoue, A., and Zhang, Y. (2011). Replication-dependent loss of 5-hydroxymethylcytosine in mouse preimplantation embryos. Science *334*, 194.

Inoue, A., Shen, L., Dai, Q., He, C., and Zhang, Y. (2011). Generation and replication-dependent dilution of 5fC and 5caC during mouse preimplantation development. Cell Res. *21*, 1670–1676.

Iqbal, K., Jin, S.G., Pfeifer, G.P., and Szabó, P.E. (2011). Reprogramming of the paternal genome upon fertilization involves genome-wide oxidation of 5-methylcytosine. Proc. Natl. Acad. Sci. USA *108*, 3642–3647.

Ito, S., Shen, L., Dai, Q., Wu, S.C., Collins, L.B., Swenberg, J.A., He, C., and Zhang, Y. (2011). Tet proteins can convert 5-methylcytosine to 5-formylcytosine and 5-carboxylcytosine. Science *333*, 1300–1303.

Jiang, L., Zhang, J., Wang, J.J., Wang, L., Zhang, L., Li, G., Yang, X., Ma, X., Sun, X., Cai, J., et al. (2013). Sperm, but not oocyte, DNA methylome is inherited by zebrafish early embryos. Cell *153*, 773–784.

Kobayashi, H., Sakurai, T., Imai, M., Takahashi, N., Fukuda, A., Yayoi, O., Sato, S., Nakabayashi, K., Hata, K., Sotomaru, Y., et al. (2012). Contribution of intragenic DNA methylation in mouse gametic DNA methylomes to establish oocyte-specific heritable marks. PLoS Genet. *8*, e1002440.

Kohli, R.M., and Zhang, Y. (2013). TET enzymes, TDG and the dynamics of DNA demethylation. Nature *502*, 472–479.

Laird, C.D., Pleasant, N.D., Clark, A.D., Sneeden, J.L., Hassan, K.M., Manley, N.C., Vary, J.C., Jr., Morgan, T., Hansen, R.S., and Stöger, R. (2004). Hairpin-bisulfite PCR: assessing epigenetic methylation patterns on complementary strands of individual DNA molecules. Proc. Natl. Acad. Sci. USA *101*, 204–209.

Li, Y., and Sasaki, H. (2011). Genomic imprinting in mammals: its life cycle, molecular mechanisms and reprogramming. Cell Res. *21*, 466–473.

Li, J.Y., Pu, M.T., Hirasawa, R., Li, B.Z., Huang, Y.N., Zeng, R., Jing, N.H., Chen, T., Li, E., Sasaki, H., and Xu, G.L. (2007). Synergistic function of DNA methyltransferases Dnmt3a and Dnmt3b in the methylation of Oct4 and Nanog. Mol. Cell. Biol. *27*, 8748–8759.

Mayer, W., Niveleau, A., Walter, J., Fundele, R., and Haaf, T. (2000). Demethylation of the zygotic paternal genome. Nature *403*, 501–502.

Meissner, A., Gnirke, A., Bell, G.W., Ramsahoye, B., Lander, E.S., and Jaenisch, R. (2005). Reduced representation bisulfite sequencing for comparative high-resolution DNA methylation analysis. Nucleic Acids Res. *33*, 5868–5877.

Nakamura, T., Arai, Y., Umehara, H., Masuhara, M., Kimura, T., Taniguchi, H., Sekimoto, T., Ikawa, M., Yoneda, Y., Okabe, M., et al. (2007). PGC7/Stella protects against DNA demethylation in early embryogenesis. Nat. Cell Biol. *9*, 64–71.

Nakamura, T., Liu, Y.J., Nakashima, H., Umehara, H., Inoue, K., Matoba, S., Tachibana, M., Ogura, A., Shinkai, Y., and Nakano, T. (2012). PGC7 binds histone H3K9me2 to protect against conversion of 5mC to 5hmC in early embryos. Nature *486*, 415–419.

Ooi, S.K., and Bestor, T.H. (2008). The colorful history of active DNA demethylation. Cell *133*, 1145–1148.

Potok, M.E., Nix, D.A., Parnell, T.J., and Cairns, B.R. (2013). Reprogramming the maternal zebrafish genome after fertilization to match the paternal methylation pattern. Cell *153*, 759–772.

Reik, W., Dean, W., and Walter, J. (2001). Epigenetic reprogramming in mammalian development. Science *293*, 1089–1093.

Rohde, C., Zhang, Y., Reinhardt, R., and Jeltsch, A. (2010). BISMA—fast and accurate bisulfite sequencing data analysis of individual clones from unique and repetitive sequences. BMC Bioinformatics *11*, 230.

Rougier, N., Bourc'his, D., Gomes, D.M., Niveleau, A., Plachot, M., Pàldi, A., and Viegas-Péquignot, E. (1998). Chromosome methylation patterns during mammalian preimplantation development. Genes Dev. *12*, 2108–2113.

Saitou, M., Kagiwada, S., and Kurimoto, K. (2012). Epigenetic reprogramming in mouse pre-implantation development and primordial germ cells. Development *139*, 15–31.

Santos, F., Hendrich, B., Reik, W., and Dean, W. (2002). Dynamic reprogramming of DNA methylation in the early mouse embryo. Dev. Biol. *241*, 172–182.

Santos, F., Peat, J., Burgess, H., Rada, C., Reik, W., and Dean, W. (2013). Active demethylation in mouse zygotes involves cytosine deamination and base excision repair. Epigenet. Chromatin *6*, 39.

Schiesser, S., Hackner, B., Pfaffeneder, T., Müller, M., Hagemeier, C., Truss, M., and Carell, T. (2012). Mechanism and stem-cell activity of 5-carboxycytosine decarboxylation determined by isotope tracing. Angew. Chem. Int. Ed. Engl. *51*, 6516–6520.

Seisenberger, S., Peat, J.R., Hore, T.A., Santos, F., Dean, W., and Reik, W. (2013). Reprogramming DNA methylation in the mammalian life cycle: building and breaking epigenetic barriers. Philos. Trans. R. Soc. Lond. B Biol. Sci. *368*, 20110330.

Smallwood, S.A., Tomizawa, S., Krueger, F., Ruf, N., Carli, N., Segonds-Pichon, A., Sato, S., Hata, K., Andrews, S.R., and Kelsey, G. (2011). Dynamic CpG island methylation landscape in oocytes and preimplantation embryos. Nat. Genet. *43*, 811–814.

Smith, Z.D., Chan, M.M., Mikkelsen, T.S., Gu, H., Gnirke, A., Regev, A., and Meissner, A. (2012). A unique regulatory phase of DNA methylation in the early mammalian embryo. Nature *484*, 339–344.

Smith, Z.D., Chan, M.M., Humm, K.C., Karnik, R., Mekhoubad, S., Regev, A., Eggan, K., and Meissner, A. (2014). DNA methylation dynamics of the human preimplantation embryo. Nature *511*, 611–615.

Song, C.X., Szulwach, K.E., Dai, Q., Fu, Y., Mao, S.Q., Lin, L., Street, C., Li, Y., Poidevin, M., Wu, H., et al. (2013). Genome-wide profiling of 5-formylcytosine reveals its roles in epigenetic priming. Cell *153*, 678–691.

Tsumura, A., Hayakawa, T., Kumaki, Y., Takebayashi, S., Sakaue, M., Matsuoka, C., Shimotohno, K., Ishikawa, F., Li, E., Ueda, H.R., et al. (2006). Maintenance of self-renewal ability of mouse embryonic stem cells in the absence of DNA methyltransferases Dnmt1, Dnmt3a and Dnmt3b. Genes Cells *11*, 805–814.

Wang, L., Zhang, J., Duan, J., Gao, X., Zhu, W., Lu, X., Yang, L., Zhang, J., Li, G., Ci, W., et al. (2014). Programming and inheritance of parental DNA methylomes in mammals. Cell *157*, 979–991.

Wossidlo, M., Arand, J., Sebastiano, V., Lepikhov, K., Boiani, M., Reinhardt, R., Schöler, H., and Walter, J. (2010). Dynamic link of DNA demethylation, DNA strand breaks and repair in mouse zygotes. EMBO J. *29*, 1877–1888.

Wossidlo, M., Nakamura, T., Lepikhov, K., Marques, C.J., Zakhartchenko, V., Boiani, M., Arand, J., Nakano, T., Reik, W., and Walter, J. (2011). 5-Hydroxymethylcytosine in the mammalian zygote is linked with epigenetic reprogramming. Nat. Commun. *2*, 241.

Xie, W., Barr, C.L., Kim, A., Yue, F., Lee, A.Y., Eubanks, J., Dempster, E.L., and Ren, B. (2012). Base-resolution analyses of sequence and parent-of-origin dependent DNA methylation in the mouse genome. Cell *148*, 816–831.